

Modelling Flood Wave Propagation as a Result of Dam Piping Failure Using 2D-HEC-RAS

Mahmood J. Mohamed¹, Ibtisam R. Karim¹, Mohammed Y. Fattah¹ , Nadhir Al-Ansari^{2*} 

¹ Civil Engineering Department, University of Technology, Baghdad, Iraq.

² Civil, Environmental and Natural Resources Engineering, University of Technology, Lulea 971 87, Sweden.

Received 14 May 2023; Revised 14 August 2023; Accepted 29 August 2023; Published 01 October 2023

Abstract

In recent years, there has been a serious request for innovative, accurate approaches to be determined and controlled for dam failures. The present study aims to explore and evaluate the flood wave parameters that result from a dam break due to piping failure occurring in the body of the dam and routing the flood waves. Mosul Dam, which lies in the north of Iraq, and a reach of the Tigris River downstream the dam to Samarra Barrage at about 470 km are selected as a case study. A two-dimensional Hydrologic Engineering Center River Analysis System (2D HEC-RAS) and the Geographic Information System (GIS) have been supposed to be suitable for development calculations of the flood wave parameters based on the Digital Elevation Model (DEM) and land cover satellite images that enhance the calculations. The reservoir and two-dimensional flow area are delineated and incorporated with DEM. Manning's coefficient for the whole area has been extracted according to the Land Cover satellite image, which showed that its value ranges between 0.025 to 0.037 with a correlation coefficient R^2 equal to 0.845 and 0.801 for the calibration and validation processes, respectively. The results of the scenario display a substantial performance of the maps produced from the model that represented the depth, velocity, and water surface elevation. All the maximum values of dam break parameters lie near the dam body and slightly decrease downstream. It is pre-eminent that the 2D HEC-RAS model is appropriate for analyzing and simulating the occurrence of dam breaches by visualizing the distribution of flood wave depth and velocities in two dimensions. Hence, the clear improvement in producing maps, which monitor the spread of hydrodynamic waves, gives an indication of risk areas that are threatened by inundation and aids in the formulation of emergency plans.

Keywords: 2D HEC-RAS; Mosul Dam; Flood Wave; Piping Failure.

1. Introduction

Dam failures are a common issue in a number of countries. When they happen, they can result in significant damage, loss of life, and property destruction. Catastrophic failures will cause a quick release of water from reservoirs [1]. Piping failure occurs when the water leaks across the dam at a substantial rate, causing internally eroded material to be transported outside of the dam. This occurs due to high porosities and a lack of controlled compaction, in which embankment dams are more susceptible to seepage or piping failure. Also, geotechnical structures may collapse due to high seepage pressures that remove soil material [2]. Numerous terminologies have been utilized in the texts to categorize the erosion due to seepage, and several studies have been concerned with this problem using different models.

Haltas et al. (2016) [3] utilized two numerical models for monitoring the development of the waves of flood downstream of the dam through densely populated urban areas using HEC-RAS software and FLO-2D software to

* Corresponding author: nadhir.alansari@ltu.se

 <http://dx.doi.org/10.28991/CEJ-2023-09-10-010>



© 2023 by the authors. Licensee C.E.J, Tehran, Iran. This article is an open access article distributed under the terms and conditions of the Creative Commons Attribution (CC-BY) license (<http://creativecommons.org/licenses/by/4.0/>).

simulate the flood hydrograph result from the Urkmez dam break. This study was allocated the IDHEC-RAS model for routing the waves in narrow valleys, while the second FLO-2D model is employed to monitor the spread of the waves outside of the valley sites in Istanbul and Eskisehir provinces of Turkey. The results illustrated that the maximum height of flood waves is 5 m at the border of the residential areas, and the maximum flood velocity is 3 meters per second. Furthermore, the flooded area in Eskisehir was estimated at 127 km².

Amini et al. (2017) [4] estimated the peak flood discharge under overtopping and piping conditions at Vahdat Dam, Kurdistan, Iran. The sizes of the breaches were estimated according to empirical relations, and their failure in overtopping and breaching was simulated using the HEC RAS model. The peak discharges were calculated using the two failures stated and monitoring the downstream flood waves. The conclusion from this study displayed the suitable potential of the HEC-RAS program in the simulation of the dam failure matter for representing the pair of failure's model. Albu et al. (2020) [5] highlighted the theoretical breaching in Sulit dam, lies on Sitna river, in Botos, Romania, and the risk results. The authors applied 2D HEC-RAS software to treat numerous dimension breaches in Sulit within a complex floodplain situation hydro morphometric parameters' computation (flood rates, flood times, height of the wave, and velocity waves). The study showed the potential of the two-dimensional model for the expected damage evaluation of the buildings and land use categories that were exposed to the damage.

Ongdas et al. (2020) [6] focused on identifying the inundation areas during flooding in a pilot project on the River Yesil by adopting the hydrodynamic model within 2DHEC-RAS. Numerous flood scenarios were implemented with multi-cell sizes (25, 50, and 75 m). The outcomes noted indicate that there are no significant changes in model performance. The risk maps established the locations that were more exposed to flooding.

Kumer et al. (2020) [7] employed the numerical model (HEC-RAS) and the Global Flood Monitoring System (GFMS) tool to model the flood in India, near the confluence of the Ganga and Yamuna Rivers. The articles established methodology for determining flood extent and making strategies for a disaster response in flood-affected areas.

Mohammed et al. (2020) [8] simulated the break of the Haditha dam that lies on the Euphrates River. The HEC-RAS model was applied in this study based on Saint-Venant equations. The results showed that the maximum discharge is 202547 m³/s at Haditha dam, and the minimum discharge is 111340 m³/s downstream. The study indicates that the elevation of the flood wave takes a longer period to reach its highest value and then decreases to its lowest level in locations far from the body of the dam. Harsanto et al. (2021) [9] studied the effect of flood waves on the bed and bank of the Winongo River by using 1D-HEC-RAS. The results showed that the maximum depth of erosion reached 0.96m. Moreover, damage to the retaining wall occurs due to erosion.

Sarchani et al. (2021) [10] estimated the flood wave in a small basin located in Northwest Crete following a rainfall event. They utilized a pair of high-resolution Digital Elevation Models within the HEC-RAS software in both one and two dimensions. Additionally, flow hydrographs were employed to determine the extent of the flooded area. The study provided valuable insights into the floodplain's extent by combining 1D and 2D models. Moreover, modeling with a Digital Elevation Model with a 2-meter resolution demonstrated clearer outputs for water depth and inundated floodplains. In another study, Karim et al. (2021) [11] analyzed the effects of hypothetical failures of the Al-Udhaim dam, specifically focusing on the overtopping scenario and the propagation wave of the flood downstream along a stretch of the Tigris River, approximately 101 kilometers from the dam. They utilized 2D HEC-RAS software to model the flood wave. The outcomes revealed approaches to assessing the extent of the flood and highlighted the significance of dam failure as a critical concern.

Hosseinzadeh-Tabrizi et al. (2022) [12] simulated piping and overtopping failures occurring in the Sattarkhan dam, located in northwestern Iran, and monitored the effects of flood waves on A-Har city using 2D HEC-RAS software. The study aimed to predict potential catastrophes in population centers downstream of the Sattarkhan dam. In another study, Mo et al. (2023) [13] investigated breach failures in earth-rock dams located along the Chengbi River. They employed a 1D HEC-RAS model for three breach scenarios (full, half, and one-third). The research demonstrated that a 1-meter rise in Water Surface Elevation (WSE) led to an almost 7% increase in flood discharge and delayed the time of peak flow by 1.5 hours.

Paşa et al. (2023) [14] investigated potential failures in two consecutive dams: a first buttress dam (concrete) and a second gravity dam (earth-fill). These dams are situated near a busy highway and a densely populated residential area. The researchers utilized 2D HEC-RAS software to analyze the risks associated with these dams. The maps generated by this model provided valuable insights into high-risk regions and identified the worst-case scenario, which could lead to damage to buildings. In a similar study, Mohamed et al. (2023) [15] employed 2D HEC-RAS software to conduct sensitivity analysis and assess the impact of different material types on breach dimensions in a virtual dam. The research highlighted the significant influence of soil type on breach dimensions. Furthermore, the study revealed a linear relationship between the reduction ratios of water storage capacity and breach width, as well as the time taken for the breach to occur.

In the present study, Mosul Dam and a reach of the Tigris River between Mosul Governorate and Samarra Barrage in the northern part of Iraq are taken as a case study. The study aims to: 1) investigate the process of the Mosul dam

break due to piping failure analysis using 2D HEC-RAS software; and 2) obtain flood inundation maps to examine the propagation of the flood wave caused by a hypothetical piping failure in Mosul dam downstream the dam to Samarra barrage and determine the variation of the depth, velocity, water surface elevation, and flood wave arrival time.

2. Description of the Study Area

The area of the study is situated within (43–45) longitude and latitude (36–38) between Mosul dam north of Iraq and extend south downstream Tigris River ending at Samarra Barrage, with a distance of about 479 kilometers from Mosul dam containing two tributaries that feed the main river with a constant discharge (the Great Zab River and the Lesser Zab River), as displayed in Figure 1 [16]. Mosul Dam is considered one of the massive hydraulic constructions found in Iraq, sited 80 km from the Iraq-Turkey border. It was constructed of a massive rock with a length of 3600 m and a height of 113 m, at a crest level of 341 m above the water surface level. The concrete spillway lies on the left abutment of the dam, with five radial gates measuring $13.5 \text{ m} \times 13.5 \text{ m}$ that release 12.600 cubic meters per second. The storage capacity of the Mosul reservoir is $1.1 \times 10^6 \text{ ha-m}$ at the normal operation level. It was noted that the average monthly discharge of the Tigris River from 1931 to 2019 was $631 \text{ m}^3/\text{s}$. The highest discharge recorded in April 1954 was $3514 \text{ m}^3/\text{s}$. Figure 2 explains the other design details of the dam [17].

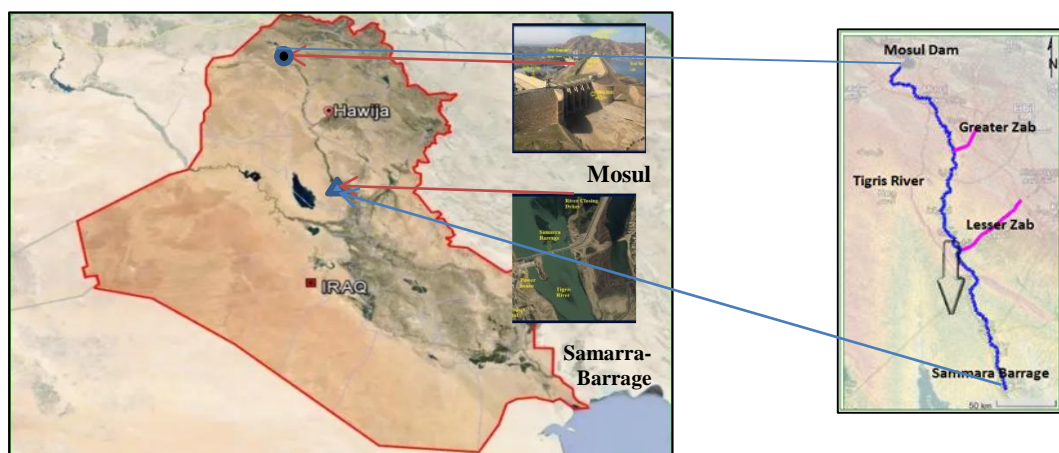


Figure 1. The study area's location

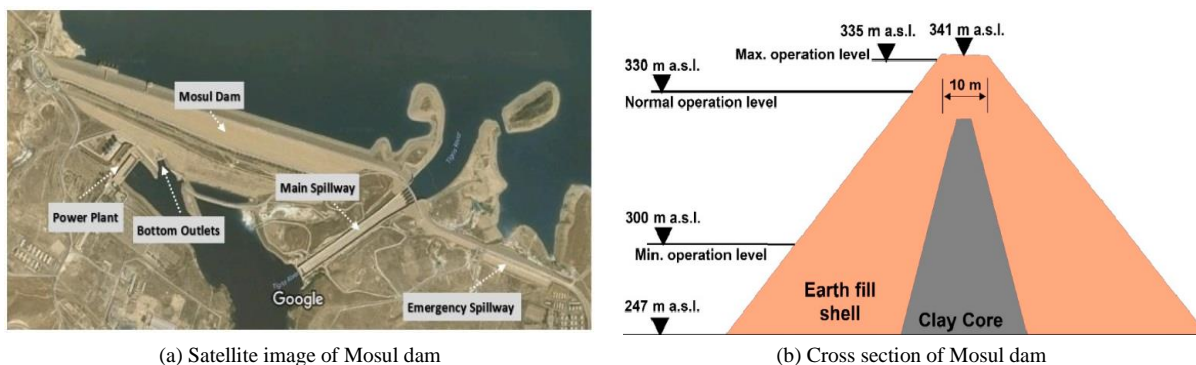


Figure 2. Mosul dam layout

3. Material and Method

3.1. Data Collection and Processing

There are two main categories of data in this study: geographic data, providing a physical description of the case study area, and flow data, offering details on river flow [18]. Initially, the Digital Elevation Model (DEM) was generated using the Shuttle Radar Topography Mission (SRTM), with grid cells measuring 14 meters. The DEM revealed the topography of the northern region of Mosul dam, characterized by high elevation near the Iraq-Turkey border, encompassing extensive mountainous terrain that gradually transitions into flat plains when moving south, as depicted in Figure 3. The selection of this study area is significant due to its inclusion of two major cities, Mosul and Tikrit. These cities are highly vulnerable to flooding in the event of Mosul dam failure, making them prone to flood risk. The study area falls within the influence of flood waves. Soil composition and land cover data for the study area were obtained from the US Geological Survey (USGS) [19]. The bed slope of the Tigris River is 0.00041, and the first quarter of the river features high banks with steep side slopes in Tikrit city [20]. Flow data, particularly water level in the reservoir and Probable Maximum Flood (PMF), are illustrated in Figure 4 [21].

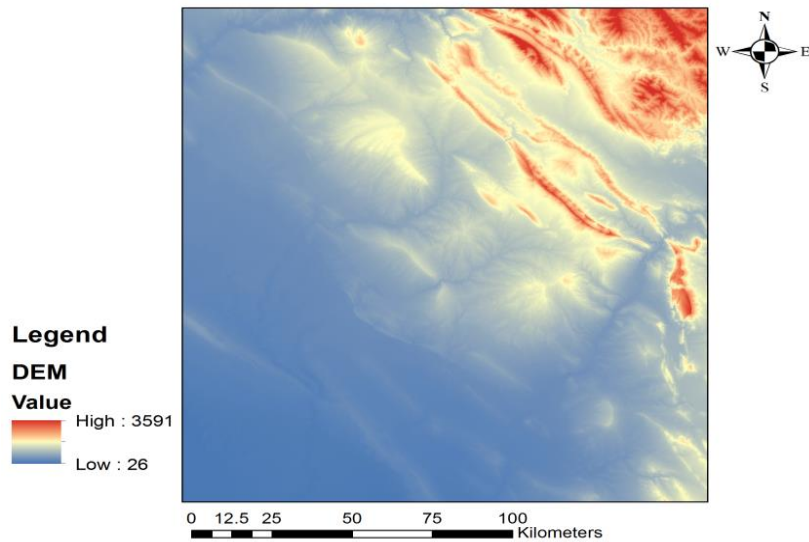


Figure 3. Digital Elevation Model (DEM) of study area

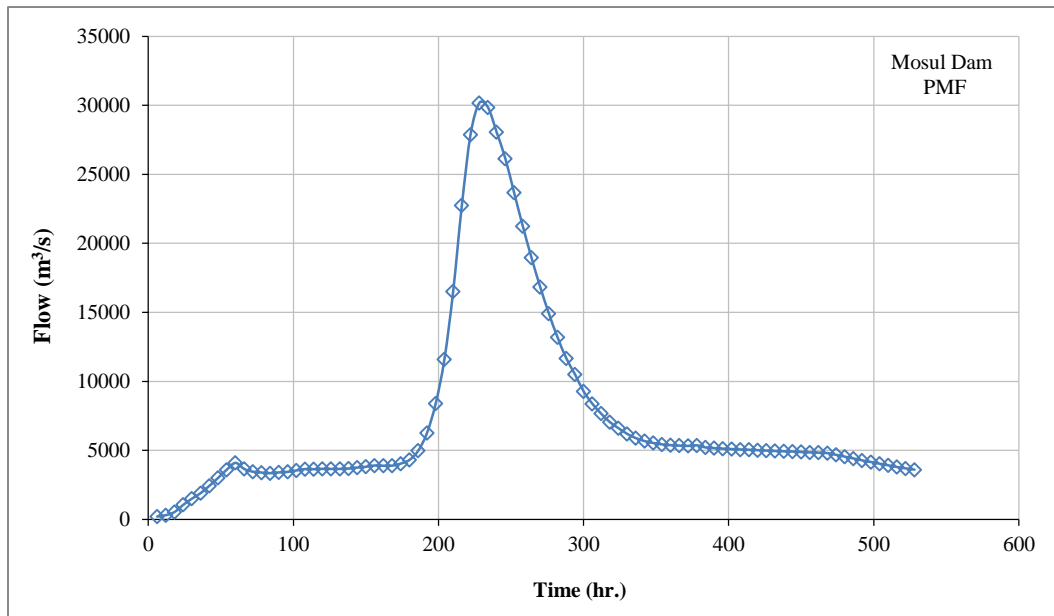


Figure 4. Probable Maximum Flood (PMF) of Mosul dam

3.2. Numerical Simulation

The HEC-RAS model components are divided into four main categories: steady flow water surface profile calculations, transport of moveable boundary sediment in quasi-unsteady, fully-unsteady, and unsteady flow's calculations, and the quality of water analysis in one and two dimensions [22]. After collecting the data required, a pair of submodels are employed within the 2D HEC-RAS software: (dam break and hydrodynamic) submodel [23]. It is first used to estimate breach parameters and derive the hydrograph of the breach. The breach parameters, such as depth, width, and side slope angles overall, as well as how long it takes for a breach to develop the final shape, are considered essential breach parameters for dam failure. Figure 5 describes these criteria [24]. Several empirical equations were utilized to estimate these parameters; among them, the Froehlich 2008 equation is stated to be the most suitable for predicting the breach parameters [25]. These equations are:

$$B_{avg}=0.27 K_O V_w^{0.32} H_b^{0.04} \tag{1}$$

$$t_f=0.0176(V_w/gH_b^2)^{0.5} \tag{2}$$

where B_{avg} is the average width of breach (m), K_O is factor equal 1 for piping failure, V_w is amount of reservoir volume above the breach's bottom level (m^3), H_b is the vertical distance between crest of the dam and the breach invert (m), t_f is time in hr, and g is gravity (m/s^2).

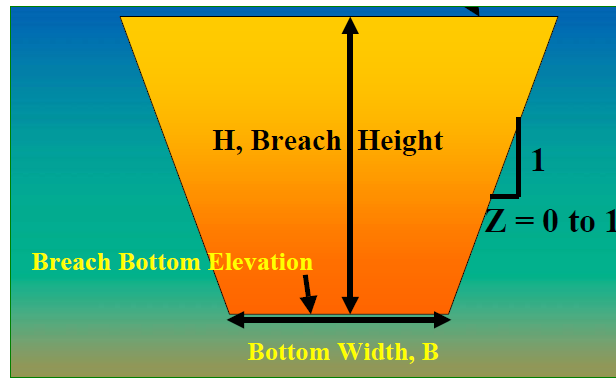


Figure 5. Scheme illustrates dam breach parameters

The second model (hydrodynamic model) is used to route the flood wave downstream from the dam termed 2D Navier Stock equations that simplified by a combination the continuity and momentum equations as stated [26, 27].

$$\frac{\partial H}{\partial t} + \frac{\partial(hu)}{\partial x} + \frac{\partial(hv)}{\partial y} + q = 0 \tag{3}$$

$$\frac{\partial u}{\partial t} + \frac{u}{\partial x} \frac{\partial u}{\partial x} + \frac{v}{\partial y} \frac{\partial u}{\partial y} = -g \frac{\partial H}{\partial x} + vt \left(\frac{\partial^2 u}{\partial x^2} + \frac{\partial^2 u}{\partial y^2} \right) - C_f u + f v \tag{4}$$

$$\frac{\partial v}{\partial t} + \frac{u}{\partial x} \frac{\partial v}{\partial x} + \frac{v}{\partial y} \frac{\partial v}{\partial y} = -g \frac{\partial H}{\partial y} + vt \left(\frac{\partial^2 v}{\partial x^2} + \frac{\partial^2 v}{\partial y^2} \right) - C_f v + f u \tag{5}$$

where H is Water Surface Elevation (L), h is depth of flood (L), u and v are the velocity element two dimensions (L/T), q is flux sink/ source (L²T⁻¹), g is gravity (LT⁻²) vt is Horizontal eddy viscosity coefficient, C_f is Bottom friction coefficient, and f is Coriolis parameter (T⁻¹).

3.3. Methodology

Initially, the flood hydrograph is computed and stated it as a boundary condition in upstream for the next model to evaluate the spreading of water surface elevation, depth, and velocity at the flooded areas. Simulating steps require gathering of the dam properties such as type of materials of the dam body, its height, length, and capacity of its reservoir. As well as, Manning's roughness coefficient, initial and boundary conditions, and the Digital Elevation Model's image are all prepared. Figure 6 illustrated the flow chart of the methodology.

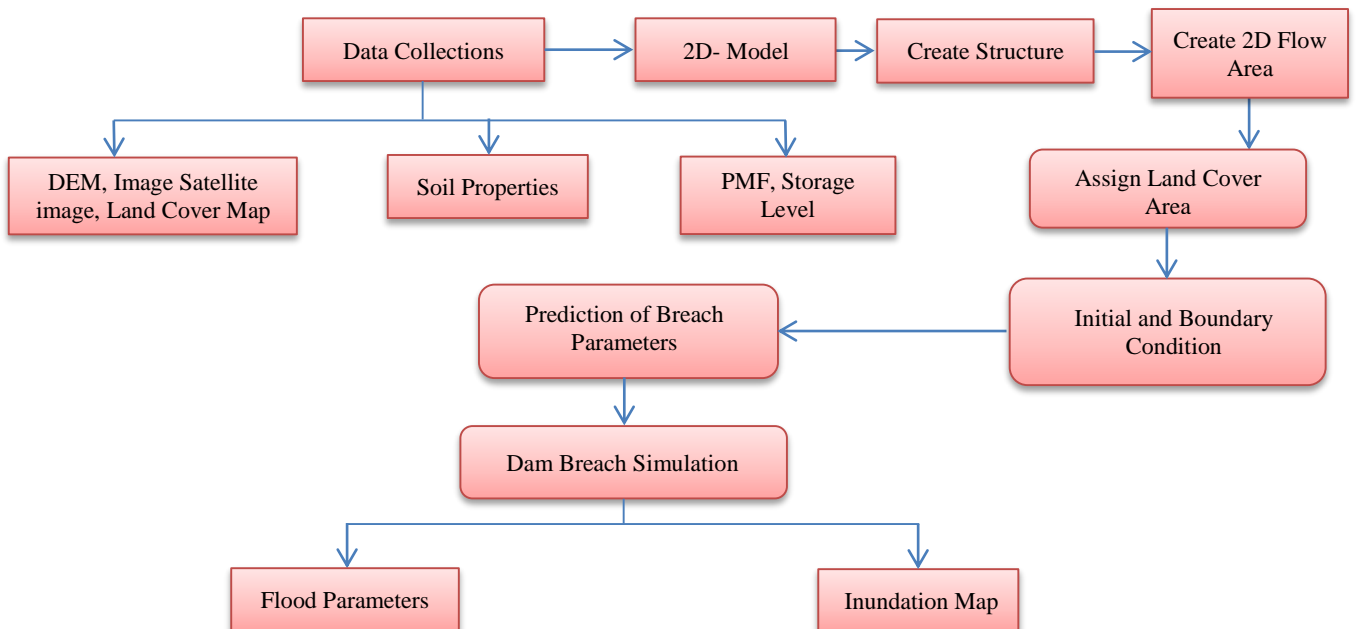


Figure 6. Flow chart of dam breach

3.4. 2D HEC-RAS –Mapper Processing

It is essential to construct a Terrain Model in RAS Mapper for any model calculations in 2D flow areas. The DEM with a 14 m resolution obtained from the Mission for Shuttle Radar Topography is converted to a triangular irregular network. The 2D flow area and the reservoir of Mosul Dam are represented according to Google's map with a cell size

of 100 m × 100 m. Manning’s roughness coefficient (n) values associated with a whole land cover type are listed in Table 1 and Figure 7. Also, the soil layer is imported into the RAS mapper, which is classified into five types (clay, clay loam, sand, sandy silt, and loamy).

Table 1. Manning’s roughness coefficient (n)

Land Cover Type	Barren Land	Open Water	Shrub	Open Space	High intensity	Cultivated Crops	Pastures
Manning's n-range	0.023-0.03	0.025-0.05	0.07-0.16	0.03-0.05	0.12-0.2	0.02-0.05	0.025-0.05

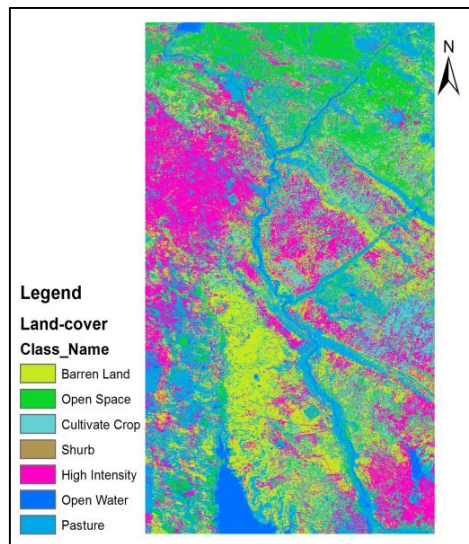
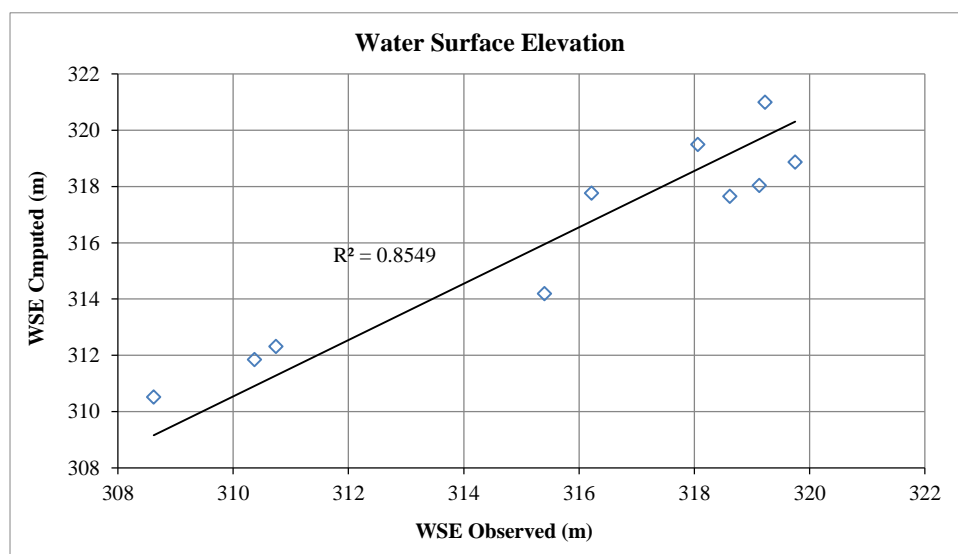


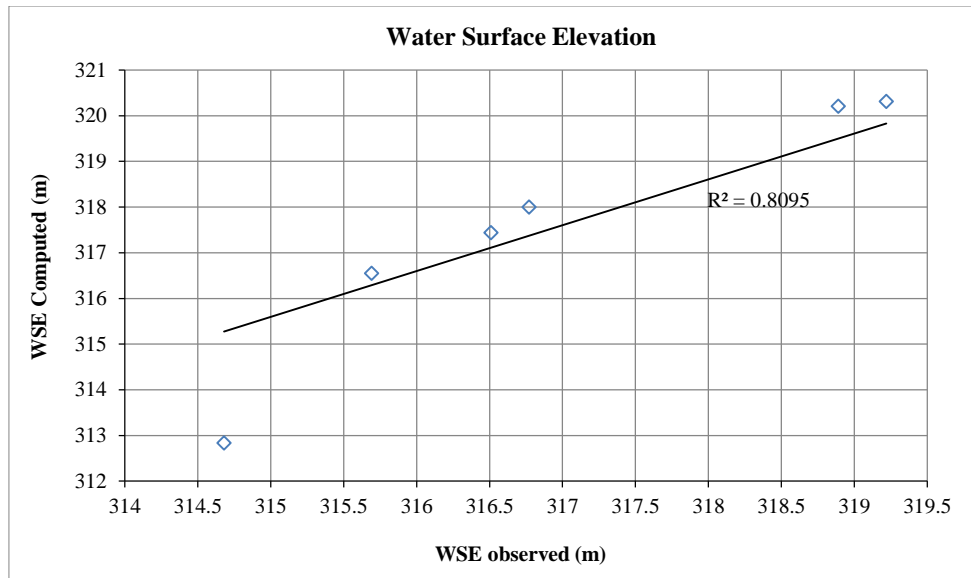
Figure 7. Land covers classification

3.5. Model Calibration and Validation

The error reduction in computing the water level values and discharges may require calibrating Manning’s roughness coefficient (n) values by setting suitable values for the main channel and the floodplain to converge the computed values compared with observed data. Several values of observed discharges in the Tigris River for the years 2003–2019 have been obtained, according to the Ministry of Water Resources [28] at the Mosul hydrological station. Twenty-one trial-and-error iterations have been implemented in 2D HEC-RAS software through utilizing a technique within the model that can be used for the calibration and validation processes based on the iterating with the range values of "n" that are associated with the land cover types. Ten Tigris River flow rates varying between 500 to 9260 m³/s are applied in the calibration process, and six flows varying between 500 to 6926 m³/s are used for validation of the model. Figure 8-a displays the scatter points of the calibration, and Figure 8-b represents the validation process for the measured and simulated water surface elevation. These figures show some discrepancies between measured and simulated data, with correlation coefficients (R²) equal to 0.845 and 0.801 for the calibration and validation processes, respectively, which represent a good agreement between the computed and recorded water levels within the river reach. Table 2 summarizes the calibrated Manning’s roughness coefficients "n".



(a) Calibration



(b) Validation

Figure 8. Observed and computed WSE during the calibration and validation processes

Table 2. Calibrated Manning's roughness coefficients

Land cover Type	Barren Land	Open Water	Shrub	Open Space	High intensity	Cultivated Crops	Pastures
Area (ha)	27566	7575.72	436	1072.1	390	702.58	368.9
Initial (n)	0.023-0.03	0.025-0.05	0.07-0.16	0.03-0.05	0.12-0.2	0.02-0.05	0.025-0.05
Calibrated (n)	0.27	0.33	0.87	0.36	0.12	0.03	0.031

3.6. Initial and Boundary Condition

The required maps for the case study are loaded into RAS Mapper, specifying the 2D flow area. The simulation is initiated with an initial reservoir water level set at 330 meters. Boundary conditions are defined using a 6-hour hydrograph of the Probable Maximum Flood (PMF) from Mosul dam and normal depths of the two tributaries, Greater Zab and Lesser Zab Rivers. The cell size for the two-dimensional flow area is set at 100 meters, as depicted in Figure 9. Additionally, Figure 10 illustrates the Elevation-Volume Curve of the Mosul dam reservoir.

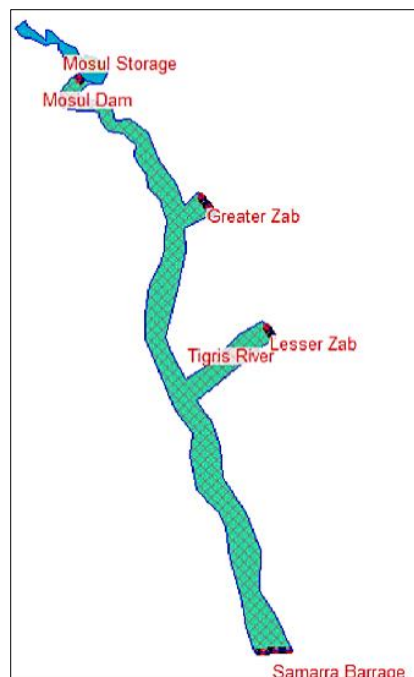


Figure 9. Reservoir storage and 2D flow area

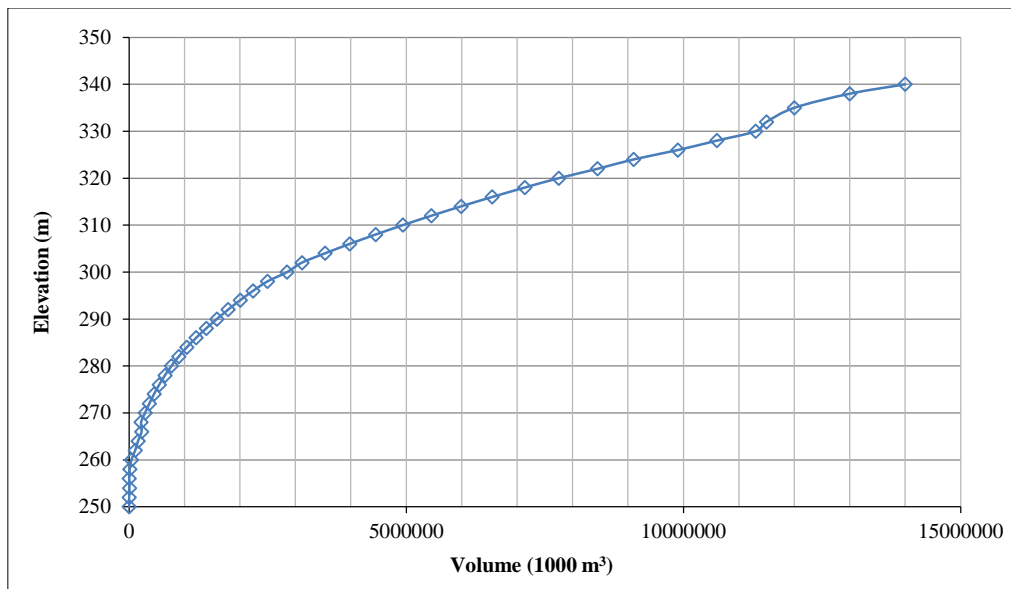


Figure 10. Elevation - Volume Curve of Mosul reservoirs

4. Results and Discussion

4.1. Results of Dam Breach Modelling

The Mosul dam breach was simulated using 2D HEC-RAS software, applying mathematical relations derived from the available dam breach mechanisms outlined in this study. The dimensions of the breach were calculated, considering the corresponding values of Manning's roughness coefficient based on the land cover type. The simulation also accounted for the lateral distribution of the flood wave along the river. Upon inputting the necessary data, the dam breach sub-model was prepared to visualize the shape of the breach caused by piping failure. The resulting top width of the breach was determined to be 477 meters, with a full breach occurring over a duration of 6.27 hours. According to Brunner [25], the side slope of the breach for piping failure is (0.7:1). Figure 11 illustrates the formed breach in the Mosul dam.

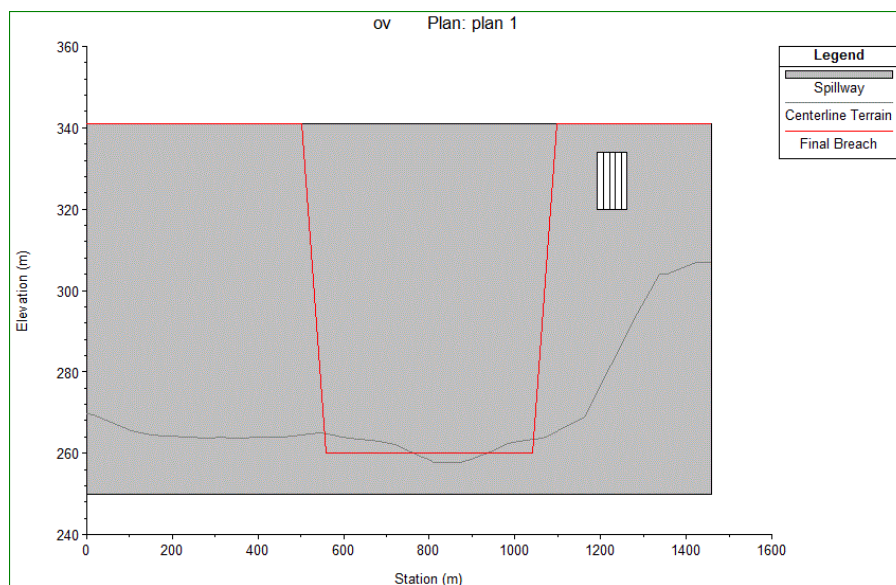


Figure 11. Details of the formed breach in Mosul dam due to piping failure

4.2. Results of the Hydrodynamic Model

The hydrodynamic model within HEC-RAS software was utilized to simulate the downstream propagation of the flood wave from Mosul dam to a distance of 479 km, terminating at Samarra barrage. The study outcomes are presented through maps visualized on the Terrain Model using RAS-Mapper in two dimensions, depicting water surface elevation (WSE), flood velocity, and wave height, as shown in Figures 12 to 14, respectively. Additionally, the profile lines illustrating flood depth, WSE, and flood velocity variations along the river in both lateral and longitudinal dimensions are displayed in Figures 15 to 17, respectively.

The simulation revealed a widespread flood flow discharge extending up to 17 km (Aski-Mosul) within a 6-hour period, as described in Figures 13-a to 13-c. The maximum depth recorded was 54 m at kilometer 5 downstream from the dam, gradually decreasing along the Tigris River (Figure 15). The spatial velocity pattern in two dimensions ranged from 1.5 to 7.5 m/s, with the highest values observed near the dam body, gradually changing along the study area, as depicted in Figures 14-a to 14-c. The results indicated that the maximum and minimum velocities were 7.02 m/s and 1.7 m/s at 5 km and 479 km, respectively (Figure 16). The extensive maps of water surface elevation are presented in Figure 15(a-c). Furthermore, the water surface elevations varied within the 2D flow area, measuring 310.71 m at kilometer 5, 205.3 m at the confluence between Greater Zab River and Tigris River (kilometer 220), 158 m at the confluence between Lesser Zab River and Tigris River (kilometer 330), and 75 m at kilometer 479 near Samarra Barrage, sequentially, as illustrated in Figure 17.

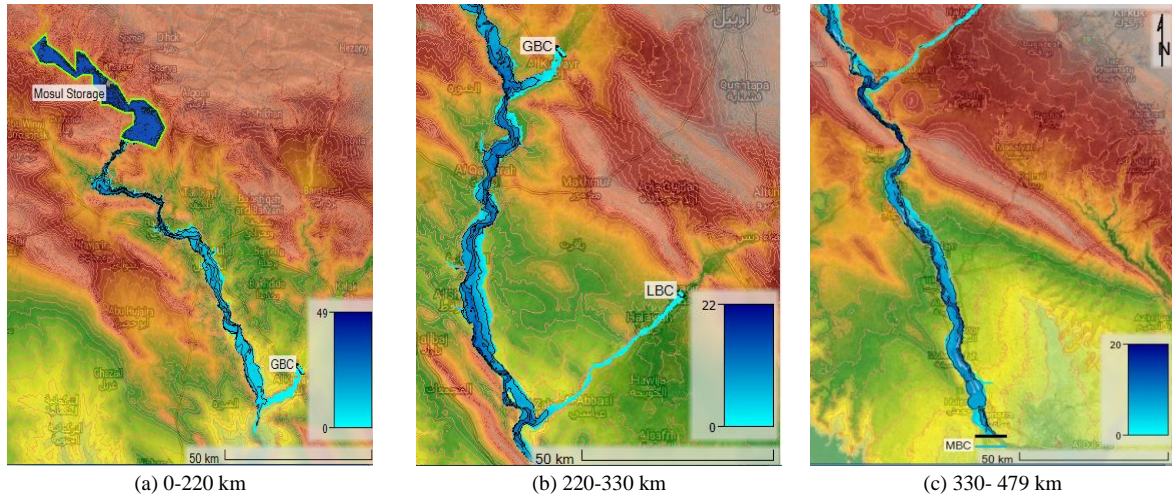


Figure 12. Flood depth distribution due to piping failure (a, b, and c)

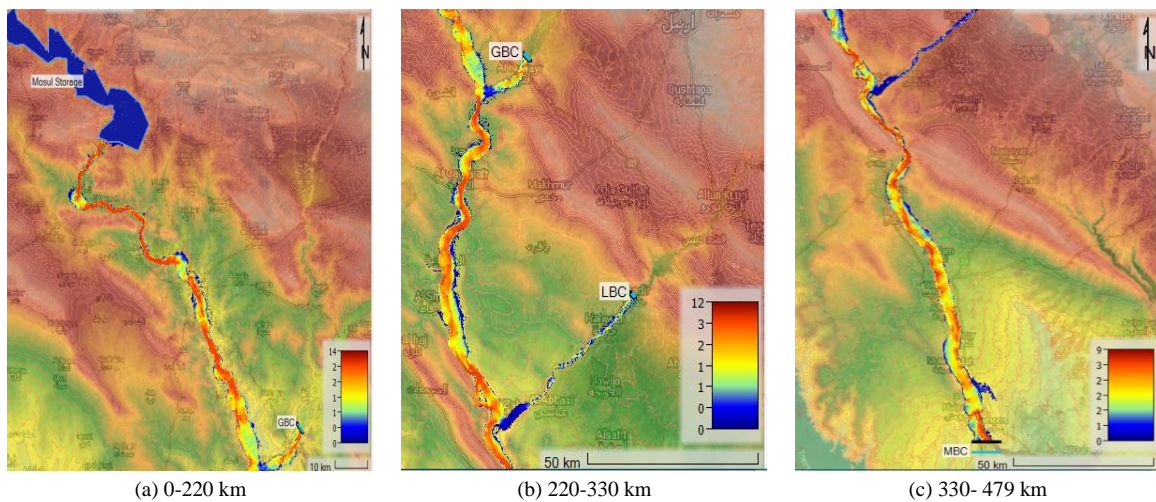


Figure 13. Flood Velocity distribution due to piping failure (a, b, and c)

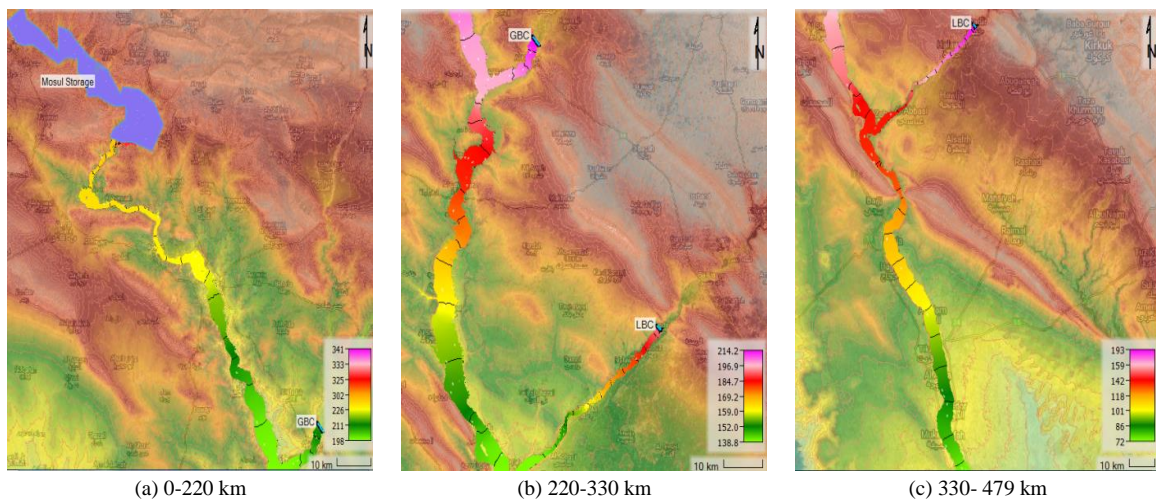


Figure 14. Water Surface Elevation Distribution due to piping failure (a, b and c)

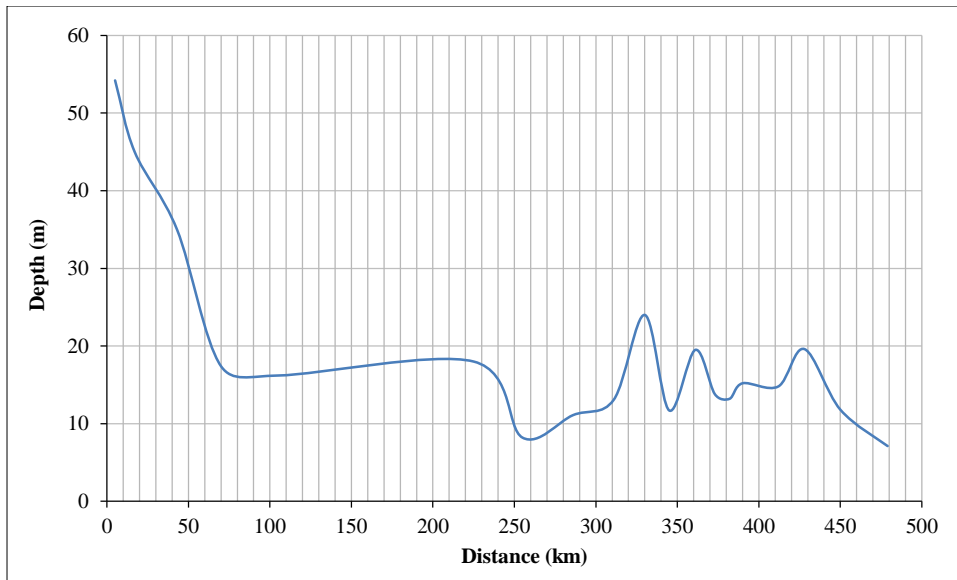


Figure 15. Profile line of the variation in water depth

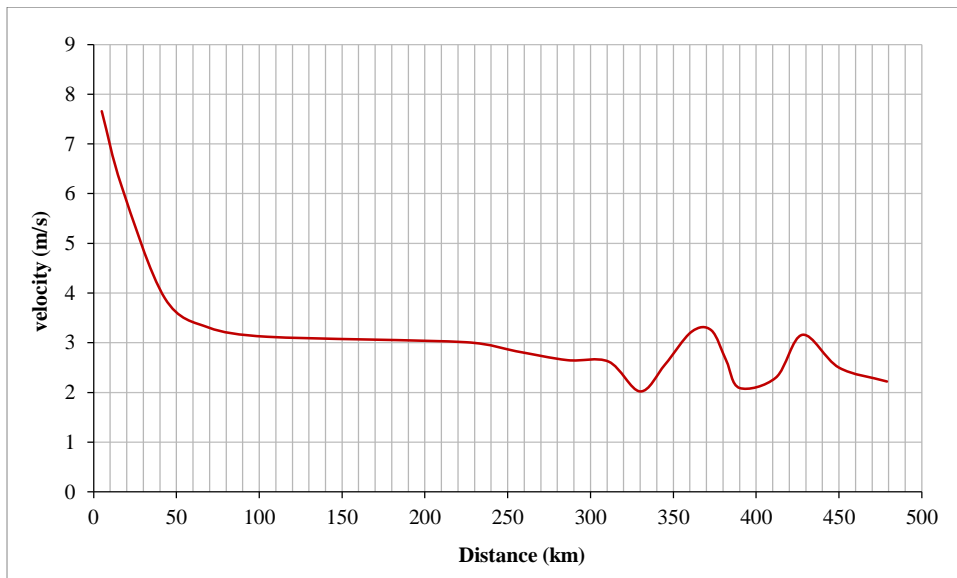


Figure 16. Profile line of the variation in water velocity

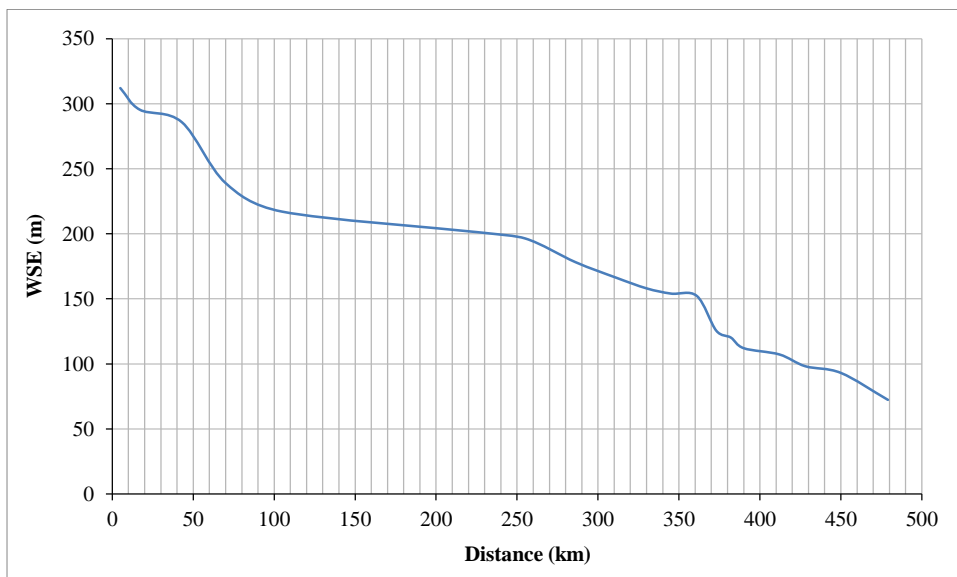


Figure 17. Profile line of the variation in water surface elevation

The maximum values of the results at different distances from the Mosul dam body to the Samarra barrage are listed in Table 3.

Table 3. Maximum dam break parameters due to piping failure

Distance (km)	Time Arrival (hr)	Depth (m)	Max velocity (m/s)	WMS (m)
5	4.4	54	7.02	310.7
17	6.1	38	5.03	285
43	7	26.2	3.5	247
70	9.1	19.4	3.84	241.6
105	13	18.1	2.51	215
225	14	17	3.61	205.3
255	19.8	8.2	2.51	193.1
286	20.7	12.8	2.73	175
311	24	14.2	2.35	167
330	26	21	2	158
356	27	19	2.1	155
361	29.3	19	6	151
373	35	12.9	2.06	124
382	36	15	1.75	118.1
390	38.4	11.8	1.85	110.1
412	40	14	2.64	106
428	42	21.6	1.85	97.2
450	44.5	14	2.5	89
479	50	8.5	1.6	75

According to the study of Al-Taiee & Rasheed [29], who examined the flood waves of many reaches in the Tigris River (in one dimension) related to the breach of the Mosul dam's failure, the results displayed that the dominant risk of flood depth occurs in Mosul city near the dam body. The reason is due to the long distance, which will cause a high loss in the energy of the wave. The present study implemented a 2D flood routing model so as to investigate the influence of the failure of the Mosul dam due to piping mode on the inundated areas, but yet no study has adopted this topic.

5. Conclusions

Since the Mosul dam has never failed historically, this study excluded calibration of the results of the breach simulation. The following points can be simply stated in light of the results from the hydraulic software:

- All critical values of dam break parameters occurred near the dam body and decreased slightly downstream. Based on the maps of the dam break parameters, it is shown that more inundation areas happen at a distance of 17 km near Aski-Mosul.
- The topographically varied conditions are largely responsible for the varying maximum flow velocity values.
- The study illustrated that the model is able to produce maps of water depth, water surface height, and flow velocity based on the visual Digital Terrain Model, which in turn makes it clear how the hydrodynamic waves spread over the study area, which aids in monitoring the flood wave and the identification of inundation areas. Meanwhile, different velocities and depths' transverse variations were represented.
- The study is meant to give a good indication of the risks that will occur and to help relevant authorities prepare plans to reduce disasters and risks resulting from floods and take the necessary measures to preserve neighboring cities, buildings, and projects before the events happen, minimizing losses as much as possible.

This study recommended further studies focus on flood wave routing probabilistic failure for Mosul dam and maneuver between reservoirs, developing risk maps for more threatened areas, and selecting control points to store the flood's water to benefit through the dry season. Also, the results of controlled experiments will be used in future studies to compare the computed data with the observed data.

6. Declarations

6.1. Author Contributions

Conceptualization, M.J.M., I.R.K., and M.Y.F.; methodology, M.J.M. and I.R.K.; validation, M.J.M., I.R.K., and M.Y.F.; investigation, I.R.K. and M.Y.F.; writing—original draft preparation, M.J.M., I.R.K., M.Y.F., and N.A.; writing—review and editing, M.J.M., I.R.K., M.Y.F., and N.A.; supervision, N.A.; funding acquisition, N.A. All authors have read and agreed to the published version of the manuscript.

6.2. Data Availability Statement

The data presented in this study are available on request from the corresponding author.

6.3. Funding

The authors received no financial support for the research, authorship, and/or publication of this article.

6.4. Acknowledgements

The authors are thankful to the Ministry of Water Recourse in Iraq for providing the data.

6.5. Conflicts of Interest

The authors declare no conflict of interest.

7. References

- [1] Luo, Y., Chen, L., Xu, M., & Tong, X. (2012). Review of dam-break research of earth-rock dam combining with dam safety management. *Procedia Engineering*, 28, 382–388. doi:10.1016/j.proeng.2012.01.737.
- [2] Talukdar, P., & Dey, A. (2019). Hydraulic failures of earthen dams and embankments. *Innovative Infrastructure Solutions*, 4(1), 42. doi:10.1007/s41062-019-0229-9.
- [3] Haltas, I., Tayfur, G., & Elci, S. (2016). Two-dimensional numerical modeling of flood wave propagation in an urban area due to Ürkmez dam-break, İzmir, Turkey. *Natural Hazards*, 81(3), 2103–2119. doi:10.1007/s11069-016-2175-6.
- [4] Amini, A., Arya, A., Eghbalzadeh, A., & Javan, M. (2017). Peak flood estimation under overtopping and piping conditions at Vahdat Dam, Kurdistan Iran. *Arabian Journal of Geosciences*, 10(6), 127. doi:10.1007/s12517-017-2854-y.
- [5] Albu, L. M., Enea, A., Iosub, M., & Breaban, I. G. (2020). Dam breach size comparison for flood simulations. A HEC-RAS based, GIS Approach for Dracsani Lake, Sitna river, Romania. *Water (Switzerland)*, 12(4), 1090. doi:10.3390/W12041090.
- [6] Ongdas, N., Akiyanova, F., Karakulov, Y., Muratbayeva, A., & Zinabdin, N. (2020). Application of HEC-RAS (2D) for Flood Hazard Maps Generation for Yesil (Ishim) River in Kazakhstan. *Water*, 12(10), 2672. doi:10.3390/w12102672.
- [7] Kumar, N., Kumar, M., Sherring, A., Suryavanshi, S., Ahmad, A., & Lal, D. (2020). Applicability of HEC-RAS 2D and GFMS for flood extent mapping: a case study of Sangam area, Prayagraj, India. *Modeling Earth Systems and Environment*, 6(1), 397–405. doi:10.1007/s40808-019-00687-8.
- [8] Mohammed, L. A., Khassaf, S. I., & Al-Murshidi, K. R. (2019). Application HEC-RAS Model to Simulate the Flood Wave Due to Dam Failure. 4th Scientific International Conference Najaf (SICN). doi:10.1109/sicn47020.2019.9019369.
- [9] Harsanto, P., Nursetiawan, Kamiel, B. P., & Cahyani, I. (2021). Riverbed Erosion Analysis of Winongo River Using HEC-RAS 5.0.7. *IOP Conference Series: Earth and Environmental Science*, 933(1), 012026. doi:10.1088/1755-1315/933/1/012026.
- [10] Sarchani, S., Seiradakis, K., Coulibaly, P., & Tsanis, I. (2020). Flood inundation mapping in an ungauged basin. *Water (Switzerland)*, 12(6), 1532. doi:10.3390/W12061532.
- [11] Karim, I. R., Hassan, Z. F., Abdullah, H. H., & Alwan, I. A. (2021). 2D-Hec-Ras Modeling of Flood Wave Propagation in a Semi-Arid Area Due to Dam Overtopping Failure. *Civil Engineering Journal*, 7(9), 1501–1514. doi:10.28991/cej-2021-03091739.
- [12] Hosseinzadeh-Tabrizi, S. A., Ghaeini-Hessaroyeh, M., & Ziaadini-Dashtekhaki, M. (2022). Numerical simulation of dam-breach flood waves. *Applied Water Science*, 12(5), 1–9. doi:10.1007/s13201-022-01623-5.
- [13] Mo, C., Shen, Y., Lei, X., Ban, H., Ruan, Y., Lai, S., Cen, W., & Xing, Z. (2023). Simulation of one-dimensional dam-break flood routing based on HEC-RAS. *Frontiers in Earth Science*, 10, 1–15. doi:10.3389/feart.2022.1027788.
- [14] Paşa, Y., Peker, I. B., Hacı, A., & Gülbaz, S. (2023). Dam failure analysis and flood disaster simulation under various scenarios. *Water Science and Technology*, 87(5), 1214–1231. doi:10.2166/wst.2023.052.

- [15] Mohamed, M., Karim, I., & Fattah, M. (2023). Impact of Dam Materials and Hydraulic Properties on Developing the Breaching Dimensions. *Engineering and Technology Journal*, 41(5), 716–723. doi:10.30684/etj.2023.138009.1368.
- [16] Ministry of Water Resource in Iraq. (2019). General directorate of water resources management, hydrological studies center, Baghdad, Iraq.
- [17] Al-Ansari, N., Adamo, N., Al-Hamdani, M. R., Sahar, K., & Al-Naemi, R. E. A. (2021). Mosul Dam Problem and Stability. *Engineering*, 13(03), 105–124. doi:10.4236/eng.2021.133009.
- [18] Alwan, I., Majeed, Z., & Abbas, A. (2021). Water Flow Simulation of Tigris River Between Samara and Baghdad Based on HEC-RAS Model. *Engineering and Technology Journal*, 39(12), 1882–1893. doi:10.30684/etj.v39i12.1804.
- [19] USGS (2023). Website Metadata from Satellite Image. Available online: <http://glovis.usgs.gov> (accessed on September 2023).
- [20] Nama, A. H., Abbas, A. S., & Maatooq, J. S. (2022). Field and Satellite Images-Based Investigation of Rivers Morphological Aspects. *Civil Engineering Journal (Iran)*, 8(7), 1339–1357. doi:10.28991/CEJ-2022-08-07-03.
- [21] EM 1110-2-1146. (1993). *River Hydraulics. Engineer Manual*, US Army Corps of Engineers (USACE), Washington, United States.
- [22] Mhmood, H. H., Yilmaz, M., & Sulaiman, S. O. (2023). Simulation of the flood wave caused by hypothetical failure of the Haditha Dam. *Journal of Applied Water Engineering and Research*, 11(1), 66–76. doi:10.1080/23249676.2022.2050312.
- [23] Altawash, M. M., & Al Thamiry, H. A. (2022). Velocity Patterns inside the Proposed Makhool Dam Reservoir with Different Operation Plans. *IOP Conference Series: Earth and Environmental Science*, 1120(1). doi:10.1088/1755-1315/1120/1/012015.
- [24] Bozkuş, Z. & Bağ, F. (2011). Virtual Failure Analysis of the Çınarcık Dam. *Teknik Dergi*, 22 (110), 1537-1549.
- [25] Froehlich, D. C. (2008). Embankment Dam Breach Parameters and Their Uncertainties. *Journal of Hydraulic Engineering*, 134(12), 1708–1721. doi:10.1061/(asce)0733-9429(2008)134:12(1708).
- [26] Brunner, G.W. (2016). *HEC-RAS River Analysis System. Hydraulic Reference Manual. Version 1.0.*; Hydrologic Engineering Center: Davis, California, United States.
- [27] USACE (2022). *HEC-RAS River Analysis System. User's Manual, Version 6.2*, Hydrologic Engineering Center. US Army Corps of Engineers (USACE), Washington, United States.
- [28] Ministry of Water Resources. (2020). *Records of Field Observations Data. State department of the operation of irrigation and deraigned projects*, Baghdad, Iraq.
- [29] Al-Taiee, T. M., & Rasheed, A. M. (2009). Simulation Tigris River flood wave in Mosul city due to a hypothetical Mosul dam break. *Damascus University Journal*, 25(2), 17-36.